ELSEVIER

Journal of Luminescence 79 (1998) 241–248

JOURNAL OF LUMINESCENCE

Electron trapping by self-trapped hole pairs and small rare-earth clusters in Sm-doped CaF_2

W. Beck[a,*], V.V. Fedorov[1,a], D. Ricard[a], C. Flytzanis[a], T.T. Basiev[b]

[a] *Laboratoire d'Optique Quantique du CNRS, Ecole Polytechnique, 91128 Palaiseau Cedex, France*
[b] *General Physics Institute, Vavilov Street 38, Moscow 117942, Russian Federation*

Received 28 January 1998; received in revised form 10 July 1998; accepted 10 July 1998

Abstract

In this paper we investigate the mechanisms for electron trapping, following photoionization of Sm^{2+} in γ- and non-γ-irradiated samples of Sm-doped CaF_2. Using linear absorption, fluorescence and site-selective coherent anti-Stokes Raman excitation spectroscopy, we show that the electron traps in non-γ-irradiated CaF_2 : Sm are small clusters of trivalent Sm ions. In the γ-irradiated samples, we observe the formation of self-trapped holes after photoionization, which provides us with additional evidence for the existence of self-trapped hole pairs in γ-irradiated rare-earth-doped CaF_2.

PACS: 82.50.F; 42.65

Keywords: Photoionization; Rare earth ions; Self-trapped holes

1. Introduction

The photoionization of Sm^{2+} in various hosts has attracted a great number of researchers, both because of fundamental reasons [1–5] and possible applications like frequency-domain data storage by persistent spectral hole burning [6–8]. Although, by now, photoionization is a well-investigated phenomenon in optical materials doped with divalent rare-earth (RE) ions, the trapping mechanism of the electron has rarely been the object of any research [9]. However, for applications like frequency-domain data storage by persistent photoionization hole burning [6–8,10,11], the electron trapping efficiency and the room temperature stability of the electron traps is of crucial importance.

In this paper, we investigate the electron traps in γ- and non-γ-irradiated CaF_2 : Sm. In Sections 3.1 and 3.2 we present experimental results which indicate that the γ-irradiated sample contains self-trapped hole pairs which act as electron traps and subsequently form self-trapped holes. In Section 3.3 we show by linear absorption, fluorescence and site-selective coherent anti-Stokes Raman spectroscopy (CARS) that the main electron traps in non-γ-irradiated CaF_2 : Sm are small Sm^{3+} clusters.

* Correspondence address. Department of Physics, University of California, 366 Leconte Hall, Berkeley, CA 94720-7300, USA. Tel.: +1 510 486 6054; fax: +1 510 643 8923; e-mail: wbeck@ux5.lbl.gov.

[1] On leave from The General Physics Institute, Moscow.

0022-2313/98/$ – see front matter
PII: S0022-2313(98)00045-3

2. Experimental

The high-temperature absorption spectra were obtained using a CARY 1413 spectrophotometer. The low-temperature absorption spectra were measured by dispersing the light of a 50 W halogen lamp with a JY 1/68 single monochromator, passing it through the sample and collecting the transmitted light either with a UV- or a red-sensitive photomultiplier. These low-temperature measurements were restricted to wavelengths above 270 nm due to the spectral characteristics of the source. The signal-to-noise ratio was improved by chopping the light in front of the monochromator and acquiring the signal with a lock-in amplifier. For each trace, a separate baseline was measured to minimize the effects of long-term drifts in the lamp intensity.

The exciting light for the fluorescence and the CARS measurements was produced by 2 ns dye lasers, simultaneously pumped by a frequency-doubled Nd : YAG laser at 532 nm with a repetition rate of 50 Hz. The dye laser pulses had a duration of 5 ns and a spectral width of less than $0.05\,cm^{-1}$.

The fluorescence spectra were measured by focusing the dye laser beam on the sample by a cylindrical lens and imaging the fluorescence on the entrance slit of the 68 cm monochromator. The light was detected by an infrared photomultiplier and the signal was acquired by a gated boxcar integrator. The exciting light was attenuated in front of the monochromator by choosing the adequate colored glass filters. The fluorescence lifetimes were measured with a digital oscilloscope.

For the CARS experiments, we chose the folded BOXCARS configuration to excite the sample [12]. To achieve a high signal-to-noise ratio, we used a beamsplitter in front of the sample to create a reference signal on a glass plate which showed no dipersion in the spectral region of interest. The generated anti-Stokes waves were passed through a double monochromator to filter out the exciting radiation and were detected by two identical photomultipliers. The signal and reference pulses were acquired by two boxcar integrators and divided shot by shot by a PC. The polarization geometry was chosen so that the nonresonant signal would be suppressed. The samples were cooled by a closed cycle helium refrigerator capable of attaining 8 K.

The non-γ-irradiated sample was grown by the Bridgman method under a flowing argon atmosphere. The crystal powders (purity 99.999) were outgassed under high vacuum before melting. PbF_2 was added as an oxygen scavenger. As PbF_2 and PbO volatilize at a much lower temperature than the other ingredients, it can be supposed that the final product was free of lead. The sample was colored green due to some of the Sm turning into the divalent state spontaneously. The γ-irradiated sample was also produced by the Bridgman method but without addition of PbF_2. It was grown under a fluorinated atmosphere and did not exhibit coloring after growth. To reduce some of the trivalent Sm present in the crystal, this sample was γ-irradiated at room temperature with a dose of 10 Mrad by a ^{60}Co sample. The Sm^{2+} concentrations of the samples were determined by the room temperature absorption at 617 nm [13] and the relative Sm^{3+} concentrations were checked by the optical density of 400 nm at 8 K. For the γ-irradiated sample, the Sm^{3+} concentration was 0.3 mol%, the Sm^{2+} concentration 0.0014 mol% and for the non-γ-irradiated sample the concentrations were 0.44 mol% and 0.0074 mol%.

3. Experimental results and discussion

3.1. Room temperature absorption spectra of the γ- and non-γ-irradiated samples

Curves a and b in Fig. 1 show the room temperature absorption spectra of the γ- and non-γ-irradiated sample, respectively. Both spectra exhibit the typical $4f^6 \rightarrow 4f^5 5d$ absorption transitions of Sm^{2+} in a cubic (O_h) site [13]. As the Sm^{2+} concentration differed in the two samples, they were both normalized to the 617 nm band to facilitate the comparison. Curve c in Fig. 1 was obtained by subtracting curve b from curve a. This difference spectrum shows that, in contrast to the non-γ-irradiated sample, the γ-irradiated sample contains a color center which has an absorption peak at around 245 nm with a half-width of approximately

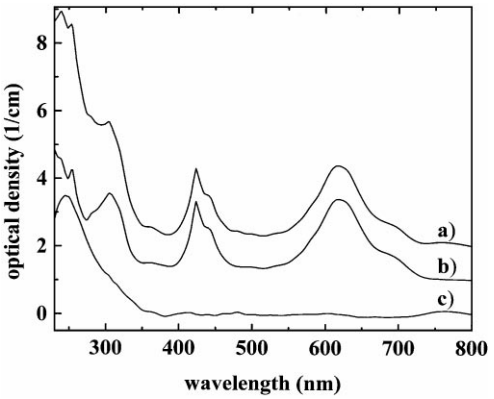

Fig. 1. Room temperature absorption spectra for the γ-irradiated (a) and non-γ-irradiated CaF_2: Sm sample (b), normalized to the 617 nm peak and the difference spectrum (c).

11 400 cm^{-1}. The same feature was observed for all samples which were available.

It is known, that ionizing radiation like γ-, X- or electron beams can produce a variety of color centers in RE-doped alkaline earth fluorides (For a short review concerning CaF_2, see Ref. [14]). This includes F-centers, multiple F-centers, metallic colloids, F-centers associated with rare-earth ions (REF centers) [15], and self-trapped holes [16]. The formation of these color centers depends on many factors like sample preparation (e.g. additive coloring) type of irradiation and sample temperature. Up to now there has been to our knowledge only one report about a color center with a single absorption line at 245 nm and a width as great as 11 400 cm^{-1} [16]. The authors of Ref. [16] observed this absorption feature in a sample of Tm-doped CaF_2 after X-irradiation at 77 K and subsequent annealing at room temperature. As a result of their experimental results, Beaumont et al. [16] postulated the formation of a self-trapped hole pair. This pair has to be considered as a neutral F_2 molecule trapped in the CaF_2 lattice. Up to now there have been only few clues for the existence of this center [16–19]. In the following section, we will present experimental results which will corroborate the interpretation that γ-irradiated CaF_2 contains self-trapped hole pairs and we will demonstrate that these centers act as efficient electron traps.

3.2. Electron trapping in the γ-irradiated sample

Curve a and b of Fig. 2 show the 8 K absorption spectra of the γ-irradiated sample before and after photoionization of Sm^{2+} in cubic sites, respectively. To bleach the sample, it was irradiated for 5 min at 10 K with the unfocused dye laser beam at 610 nm with an average power of 100 mW. The use of a pulsed laser for this experiment is justified due to the two-photon nature of the photoionization process [20]. To be able to see any changes between curves a and b apart from the evident change in the concentration of Sm^{2+} in the cubic sites, we subtracted the curve a from curve b after normalizing the former to the Sm^{2+} peak at 427 nm. The result is shown in Fig. 3a. A broad peak at 305 nm with a FWHM of 8000 cm^{-1} can be observed. The position and the width of the peak coincides with the $^2\Sigma_u \rightarrow {}^2\Sigma_g$ hole transition of the H-center in CaF_2 [21]. The H-center is a F_2^- molecular ion with one of the fluorines being an interstitial. The sharp peaks around 400 nm are due to Sm^{3+} and are visible only due to the normalization procedure. A further element, corroborating the interpretation of the peak as originating from an H-center, is the annealing of this peak. The center starts decaying at about 135 K, which corresponds to the behavior of the H-center [16].

The creation of H-centers due to electron trapping by a color center already present in the crystal has the following implication: The primary color

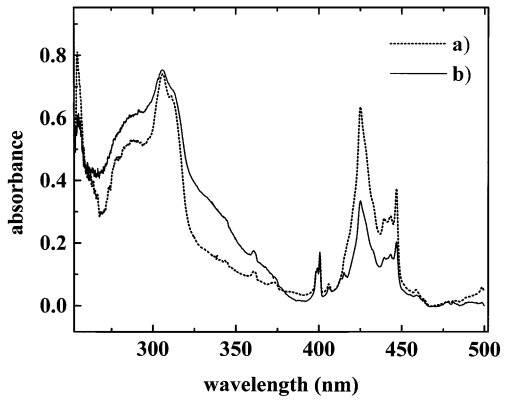

Fig. 2. Absorption spectra of the γ-irradiated sample at 8 K before (a) and after irradiation with 610 nm (b).

center plus electron has to yield an H-center which can be described as an F_2^- molecular ion. A simple explanation can be given by considering a reaction of the type: $F_2^0 + Sm^{2+} \xrightarrow{h\nu} F_2^- + Sm^{3+}$ which identifies the color center with its absorption peak at 245 nm (Fig. 1) as a F_2^0 molecule embedded in the lattice. In fact, by trapping an electron on the self-trapped hole pairs, we inverse the way this color center was encountered in previous works: In Ref. [16], the authors started with a CaF_2 sample containing only trivalent rare earth ions. Due to X-irradiation at low temperature, they created divalent RE ions and self-trapped holes (V_k- and H-centers). At higher temperatures (130 K) the V_k-centers decayed or formed H-centers and, at room temperature, they observed the formation of self-trapped hole pairs. So the final state of their sample is most probably identical to the initial state of our samples: They contain self-trapped hole pairs and divalent rare-earth ions. We trap an electron on a self-trapped hole pair to form a trivalent rare-earth ion and a self-trapped hole. The possibility of reversing the train of events corroborates the existence of self-trapped hole pairs in γ-irradiated RE-doped CaF_2.

After excitation of the $^2\Sigma_u \rightarrow {}^2\Sigma_g$ hole transition with the frequency-doubled dye laser beam at 345 nm (average power 0.01 mW) at 8 K the H-center signature decreases and the cubic Sm^{2+} concentration increases (Fig. 3b). After long irradiation

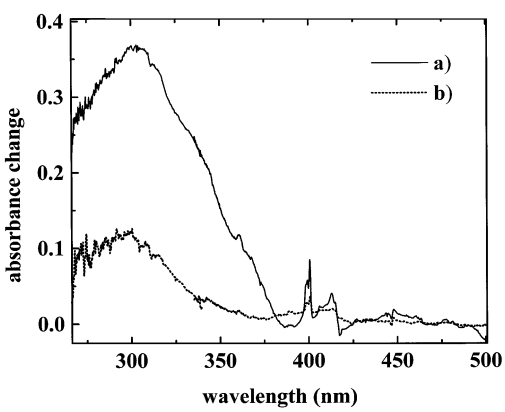

Fig. 3. Difference spectrum obtained from Fig. 2 by subtracting curve a from curve b after normalizing the former to the Sm^{2+} content after photoionization (a) after 345 nm irradiation (b).

times, the initial situation before 610 nm irradiation is almost entirely restored. This experimental fact can be explained by the excitation of the self-trapped holes into the valence band of the crystal after which they can be scattered by a Sm^{3+} in a cubic site. The F_2^- then loses its electron for the benefit of the rare earth and the result is a F_2^0 molecule and a divalent rare earth. This process made it impossible for us to register the fluorescence spectrum of the self-trapped holes, as the destruction of the F_2^- is rapid at very low excitation powers.

The possibility of creating intrinsic self-trapped holes photochemically may facilitate the investigation of their physical properties. Up to now, these small polarons were usually created by low-temperature electron- or X-irradiation. It is evident that the photochemical production of these color centers is by far the easiest method developed. An important question is, whether the self-trapped holes are impurity associated or not. The authors of Ref. [16] affirmed that in the electron–paramagnetic resonance spectra no such association could be observed. Thus, γ-irradiated $CaF_2:RE^{2+}$ may be a good system to study the intrinsic properties of self-trapped holes in alkaline earth fluorides.

3.3. Electron trapping in the non-γ-irradiated sample

3.3.1. Linear absorption spectra

The situation in the non-γ-irradiated CaF_2: Sm sample is quite different from the γ-irradiated one. Fig. 4 shows the 8 K absorption spectra of the sample in the initial state (a) and after bleaching for 5 min at 8 K with the unfocused dye laser beam at 610 nm and a power of 100 mW. (b) In order to obtain the pure electron trap spectrum free from the cubic site spectrum, we normalized curve a to the cubic Sm^{2+} concentration after photoionization and subtracted it from curve b (Fig. 5).

The difference between the spectrum in Fig. 5 and the trap spectrum of the γ-irradiated sample (Fig. 3) is evident. In respect to the unbleached sample (Fig. 4a), the bleached sample (Fig. 5) shows a red shift and a strong broadening of all the bands. As Beck et al. already showed in a previous work [22], the electron traps in this type of sample are dimers or trimers of Sm^{3+}. In particular, the

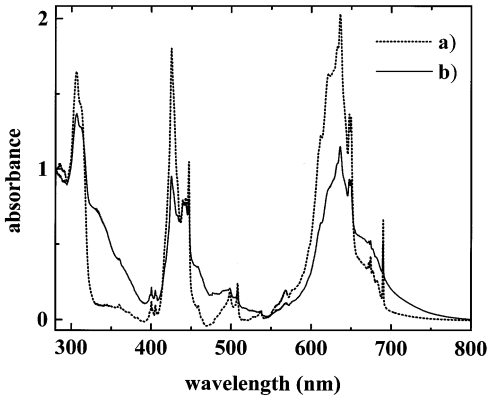

Fig. 4. Absorption spectra of the non-γ-irradiated sample at 8 K before (a) and after irradiation with 610 nm (b).

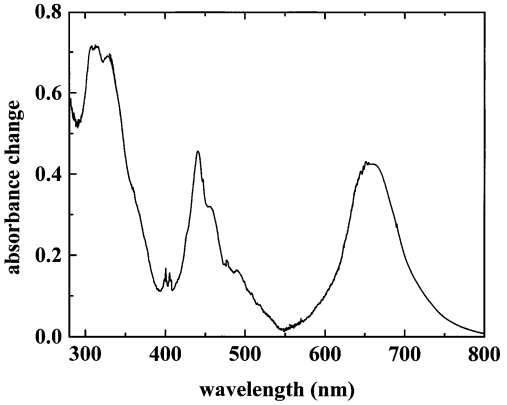

Fig. 5. Difference spectrum obtained from Fig. 4 by subtracting curve a from curve b after normalizing the former to the Sm^{2+} content after photoionization.

Raman lines originating from these clusters after electron trapping were identified due to the nearly quadratic dependence of their line strength on the Sm^{3+} concentration. To corroborate the connection of the linear absorption spectrum presented in Fig. 5 and the Raman spectrum of the traps, we use CARS and CARS-excitation spectra.

3.3.2. CARS and CARS-excitation spectra

Fig. 6 shows the polarized CARS spectrum of the non-γ-irradiated sample after red (690 nm) irradiation. The polarization geometry was chosen

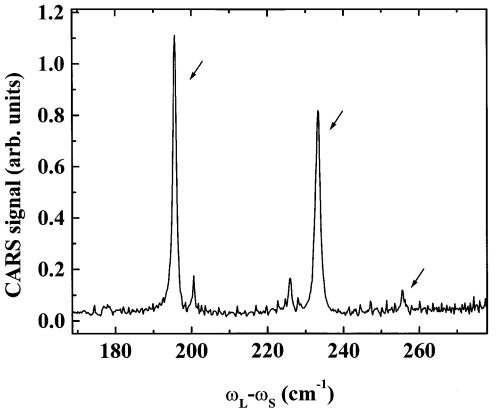

Fig. 6. Polarized CARS spectrum at 8 K of the non-γ-irradiated sample. The anti-Stokes frequency was fixed at $\lambda_{AS} = 693$ nm and both Stokes and laser wavelengths were scanned.

so as to suppress the nonresonant $\chi^{(3)}_{NR}$. In this spectrum both the input frequencies were scanned, keeping the anti-Stokes wavelength λ_{AS} fixed at 693 nm. Apart from the $^7F_0 \rightarrow {}^7F_1$ electronic Raman transition of Sm^{2+} (O_h) at 256 cm^{-1}, there are two strong lines to be seen at 195.5 and 233 cm^{-1}, which originate from an Sm^{2+} with one or more neighboring Sm^{3+}[22].

To connect the CARS and the linear absorption spectra, we make use of site-selective CARS excitation spectroscopy. The polarized CARS signal intensity in a double resonance condition, neglecting absorption, is given by the square of the resonant third-order susceptibility $\chi^{(3)}_R$[23]:

$$\chi^{(3)}_R(\omega_{AS} = \omega_L - \omega_S + \omega_L)_{ijkl} = -\frac{Ne^4}{\hbar^3}\sum_m \frac{\langle g|r_i|n'\rangle\langle n'|r_j|g\rangle}{(2\omega_L - \omega_S - \omega_{n'g} + i\Gamma_{n'g})(\omega_L - \omega_S - \omega_{g'g} + i\Gamma_{g'g})} \times \left(\frac{\langle g'|r_k|m\rangle\langle m|r_l|g\rangle}{\omega_L - \omega_{mg}} + \frac{\langle g'|r_l|m\rangle\langle m|r_k|g\rangle}{-\omega_S - \omega_{mg}}\right)\rho^0_{gg} + j \leftrightarrow l,$$

where g denotes the ground level, g' the Raman level and n' the intermediate level. The equation shows, that by fixing $\omega_L - \omega_S$ on $\omega_{g'g}$ and tuning both ω_L and ω_S so that $\omega_{AS} = 2\omega_L - \omega_S$ passes over

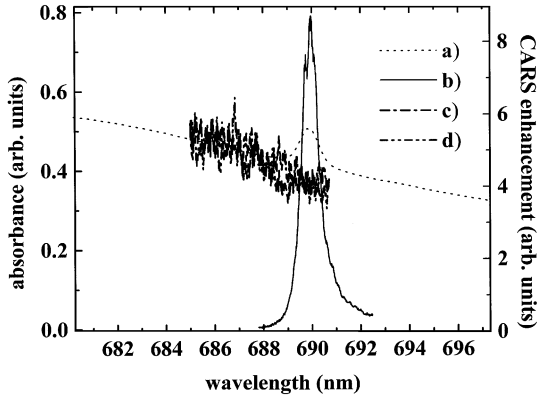

Fig. 7. The 8 K absorption spectrum of the partially bleached non-γ-irradiated sample (a), CARS excitation spectrum with $\omega_L - \omega_S = 256\,cm^{-1}$ (b), and with $\omega_L - \omega_S = 233$ (c) and $195.5\,cm^{-1}$ (d).

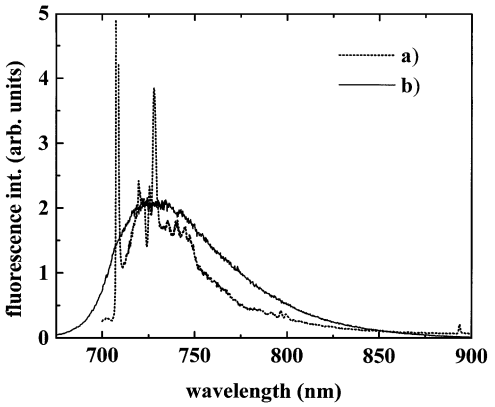

Fig. 8. The 8 K fluorescence spectrum of the unbleached non-γ-irradiated sample excited at 610 nm (a), and the fluorescence spectrum of the sample in the bleached state, excited at 580 nm (b). The zero-phonon line at 708 nm in curve a is truncated for a better visibility. The original height was 27 on the given scale.

the intermediate resonance $\omega_{n'g}$, there will be a resonance enhancement of $\chi_R^{(3)}$ due to the double resonance. As the enhancement takes place only for coupled Raman and intermediate resonances, this method can be site-selective.

Fig. 7a shows a fragment of the absorption spectrum of the sample in a partially bleached state. Curve b (CARS excitation spectrum) was obtained by fixing $\omega_L - \omega_S$ on the cubic Sm^{2+} resonance at $256\,cm^{-1}$ and curves c and d correspond to $\omega_L - \omega_S$ equal to $233\,cm^{-1}$ and $195.5\,cm^{-1}$, respectively. The small signal-to-noise ratio of curves c and d is due to the low signal intensity compared to curve b. As expected, the $256\,cm^{-1}$ line is enhanced by the $A_{1g}\,(4f^6) \rightarrow T_{1u}\,(4f^5 5d)$ transition of Sm^{2+} in the cubic site at 690 nm, but the other two Raman lines are enhanced by the broad red absorption band denoted in Fig. 5. These results show the direct connection between the electron trap lines in the CARS spectrum and the absorption spectrum shown in Fig. 5, and thus proves that Fig. 5 represents the absorption spectrum of Sm^{3+} dimers or trimers plus electron.

3.3.3. Fluorescence spectra

The difference between the bleached and unbleached (non-γ-irradiated) sample is even more striking in the fluorescence spectra. Fig. 8 shows the fluorescence spectra of the sample in the unbleached (a) and in the bleached state (b). Curve a was obtained by laser excitation at 610 nm. At this wavelength the absorption coefficient is non-zero for the traps as well as for cubic Sm^{2+} sites. As at high excitation powers, the electron traps can be reionized at this wavelength, a photochemical equilibrium is attained between the concentration of electrons trapped on Sm^{3+} clusters and of Sm^{2+} in cubic sites. Under these conditions, in Fig. 8a the sample may be slightly bleached. This effect is however of minor importance and the spectrum of Fig. 8a coincides almost perfectly with literature data [13]. The main features are the strong zero-phonon line ($A_{1u}\,(4f^5 5d) \rightarrow T_{1g}\,(4f^6)$) at 708 nm with its broad phonon sideband centered at about 725 nm. The sharp structure of the phonon wing can be explained by full symmetric vibrations of the ions of the Sm^{2+}-$8F^-$ complex [24]. The measured fluorescence lifetime is 1.05 μs. This value is slightly lower than that given in literature [25] but, as no dependence on excitation power was observed, we consider our value to be correct.

The fluorescence spectrum of the sample in the bleached state was obtained by excition at 580 nm. At this wavelength, the absorption of the electrons trapped on Sm^{3+} clusters is almost zero, so that after an irradiation time of several hours, the

fluorescence of the cubic Sm^{2+} becomes indetectable. As can be observed, the residual absorption of the traps is sufficient to record their fluorescence spectrum. In contrast to the Sm^{2+} (O_h) fluorescence, the trap spectrum exhibits only one broad band, which looks like a phonon sideband, although it is without the sharp structure of the Sm^{2+} (O_h) sideband which originates from local phonons [24]. Also, no sharp zero-phonon feature is observed. The lifetime of this fluorescence is 0.68 μs which is almost half the lifetime of Sm^{2+} in the cubic site.

As the electron-lattice phonon coupling of an Sm^{2+} incorporated in a Sm^{3+} cluster can be expected to be larger than that for an Sm^{2+} in a cubic site, the zero-phonon line may be much weaker in comparison to its phonon sideband and thus difficult to observe. The reduction of the symmetry and stronger electron–phonon coupling of Sm^{2+} in the cluster site can also explain the shorter fluorescence lifetime and the broadening of the absorption bands (denoted in Fig. 5) due to faster nonradiative relaxation rates. The shorter fluorescence lifetime is a rather common observation in RE clusters due to faster radiative and nonradiative relaxation rates [26]. It should be mentioned that the 5d orbitals of the Sm^{3+} ions in a cluster might be partly hybridized, in which case an excited electron could relax not only to the ion which was excited, but also to a neighbouring Sm^{3+}. Such photostimulated intra-cluster electron transfers may be an interesting topic for future research.

4. Summary and conclusions

Using linear absorption, fluorescence, CARS and CARS-excitation spectroscopy, we investigated the nature and properties of electron traps in γ- and non-γ-irradiated Sm doped CaF_2. The observed formation of self-trapped holes after photoionization of Sm^{2+} in γ-irradiated CaF_2:Sm provides additional experimental evidence for the existence of self-trapped hole pairs in this system. At the same time, the possibility of photochemical creation of self-trapped holes may facilitate the experimental study of their physical properties. In Section 3.3, previous observations, identifying the electron traps as small trivalent rare-earth clusters [22], were corroborated and the absorption and fluorescence of these clusters + electron were presented. The absence of the zero-phonon line in the fluorescence spectrum, the short fluorescence lifetime and the strong broadening of the absorption bands were explained by a strong coupling between the Sm^{2+} in the cluster site and the phonons of the lattice.

As in both crystals the photoionization of cubic Sm^{2+} is persistent at room temperature and the electron trap concentration can be controlled either by the γ-irradiation dose or the Sm^{3+} concentration, there is a potential for applications: It is known that in Sm doped mixed crystal systems the ratio of homogeneous and inhomogeneous spectral line widths at room temperature can be smaller than 1 at room temperature [10]. The problem of using these materials for spectral data storage may however be due to the lack or low concentration of stable electron traps. If γ-irradiation or an Sm^{3+} concentration variation have a similar effect in mixed crystals, these methods could be a simple way to introduce electron traps. This way, a multitude of mixed crystals may show persistent spectral hole-burning at room temperature, which would not be the case without the introduction of additional electron traps.

Acknowledgements

We are very thankful for many helpful discussions with A. Ya. Karasik from the General Physics Institute in Moscow.

References

[1] R.M. Macfarlane, W.S. Brocklesby, P.D. Bloch, R.T. Harley, Opt. Commun. 58 (1986) 25.
[2] C. Pedrini, F. Rogemond, D.S. McClure, J. Appl. Phys. 59 (1986) 1196.
[3] R.L. Fuller, D.S. McClure, Phys. Rev. B 43 (1991) 27.
[4] W. Mou, D.S. McClure, Phys. Rev. B 47 (1993) 11 031.
[5] R.M. Macfarlane, R.M. Shelby, Opt. Lett. 9 (1984) 533.
[6] K. Hirao, J. Non-Cryst. Solids 196 (1996) 16.
[7] A. Kurita, T. Kushida, T. Izumitani, M. Matsukawa, Opt. Lett. 19 (1994) 314.

[8] M. Nogami, Y. Abe, K. Hirao, D.H. Cho, Appl. Phys. Lett. 66 (1995) 2952.
[9] A. Winnacker, R.M. Shelby, R.M. Macfarlane, Opt. Lett. 10 (1985) 350.
[10] N. Kodama, S. Hara, Y. Inoue, K. Hirao, J. Lumin. 64 (1995) 181.
[11] W.E. Moerner, Persistent Spectral Hole-Burning: Science and Applications, Springer, Berlin, 1988.
[12] Light scattering in solids II, in: M. Cardona, G. Güntherodt (Eds.), Topics in Applied Physics, vol. 50, Springer, New York, 1982.
[13] D.L. Wood, W. Kaiser, Phys. Rev. 126 (1962) 2079.
[14] B.G. Ravi, S. Ramasamy, Int. J. Mod. Phys. B 6 (1992) 2809.
[15] D.L. Staebler, S.E. Schnatterly, Phys. Rev. B 3 (1971) 516.
[16] J.H. Beaumont, W. Hayes, D.L. Kirk, G.P. Summers, Proc. Roy. Soc. London A 315 (1970) 69.
[17] Z.J. Kiss, D.L. Staebler, Phys. Rev. Lett. 14 (1965) 691.
[18] J.L. Merz, P.S. Pershan, Phys. Rev. 126 (1967) 217.
[19] V.M. Lisitsyn, L.A. Lisitsyna, M.I. Kalinin, V.M. Reiterov, V.A. Fedorov, Opt. Spectrosc. 43 (1978) 539.
[20] J.K. Lawson, S.A. Payne, J. Opt. Soc. Am. B 8 (1991) 1404.
[21] R.T. Williams, K.S. Song, J. Phys. Chem. Sol. 51 (1990) 679.
[22] W. Beck, D. Ricard, C. Flytzanis, Appl. Phys. Lett. 69 (1996) 3197.
[23] J.-L. Oudar, Y.R. Shen, Phys. Rev. A 22 (1980) 1141.
[24] V.A. Bonch-Bruevich, I.V. Ignatev, V.V. Ovsyankin, Opt. Spectrosc. 44 (1978) 296.
[25] P.P. Feofilov, Opt. Spectrosc. 1 (1956) 992.
[26] T.P.J. Han, G.D. Jones, R.W.G. Syme, Phys. Rev. B 47 (1993) 14 706.